PROCEEDINGS OF THE ROYAL SOCIETY A MATHEMATICAL, PHYSICAL & ENGINEERING SCIENCES

Physical limitations on antennas of arbitrary shape

Mats Gustafsson, Christian Sohl and Gerhard Kristensson

Proc. R. Soc. A 2007 **463**, 2589-2607
doi: 10.1098/rspa.2007.1893

PROCEEDINGS OF THE ROYAL SOCIETY A

Proc. R. Soc. A (2007) **463**, 2589–2607
doi:10.1098/rspa.2007.1893
Published online 18 July 2007

Physical limitations on antennas of arbitrary shape

By Mats Gustafsson*, Christian Sohl and Gerhard Kristensson

Department of Electrical and Information Technology, Lund University, Sweden

In this paper, physical limitations on bandwidth, realized gain, Q-factor and directivity are derived for antennas of arbitrary shape. The product of bandwidth and realizable gain is shown to be bounded from above by the eigenvalues of the long-wavelength, high-contrast polarizability dyadics. These dyadics are proportional to the antenna volume and are easily determined for an arbitrary geometry. Ellipsoidal antenna volumes are analysed in detail, and numerical results for some generic geometries are presented. The theory is verified against the classical Chu limitations for spherical geometries and shown to yield sharper bounds for the ratio of the directivity and the Q-factor for non-spherical geometries.

Keywords: physical limitations; antennas; polarizability; scattering cross-section; dispersion relation; optical theorem

1. Introduction

The concept of physical limitations for electrically small antennas was first introduced more than half a century ago by Wheeler (1947) and Chu (1948). Since then, much attention has been drawn to the subject and numerous papers have been published (see Hansen (2006) and references therein). Unfortunately, almost all of these papers are restricted to the sphere via the spherical vector wave expansions, deviating only slightly from the pioneering ideas introduced by Chu (1948).

The objective of this paper is to derive physical limitations on bandwidth, realized gain, Q-factor and directivity for antennas of arbitrary shape. The limitations presented here generalize the classical results by Chu in many aspects. The most important advantage of the new limitations is that they no longer are restricted to the sphere but instead hold for arbitrary antenna volumes. In fact, the smallest circumscribing sphere is far from optimal for many antennas, cf. the dipole and loop antennas by Gustafsson *et al.* (2007). Furthermore, the new limitations successfully separate the electric and magnetic material properties of the antennas and quantify them in terms of their polarizability dyadics. This is the first in a series of two on physical limitations on antennas. The second paper is by Gustafsson *et al.* (2007) and illustrates the sharpness of these limitations for some classical antennas.

The new limitations introduced here are also important from a radio system point of view. Specifically, they are based on the bandwidth and the realizable gain as well as the Q-factor and the directivity. The interpretation of the

* Author for correspondence (mats.gustafsson@eit.lth.se).

Received 22 March 2007
Accepted 14 June 2007

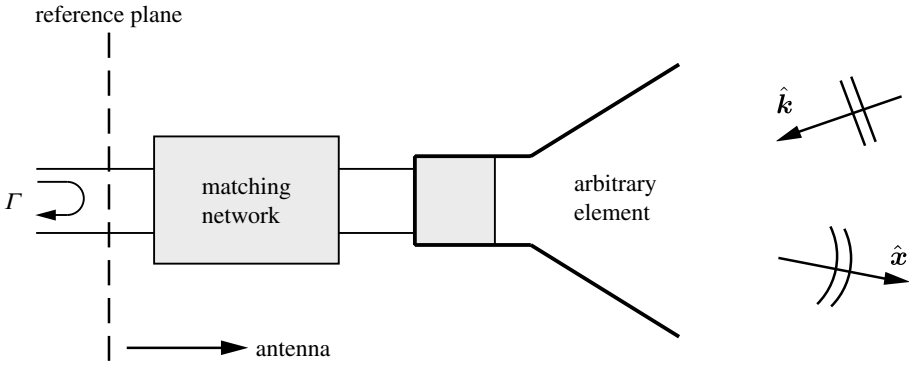

Figure 1. Illustration of a hypothetical antenna subject to an incident plane wave in the $\hat{\boldsymbol{k}}$-direction.

Q-factor in terms of the bandwidth is still subject to some research (Yaghjian & Best 2005). Moreover, the new limitations permit the study of polarization effects and their influence on the antenna performance. An example of such an effect is polarization diversity for applications in multiple input–multiple output (MIMO) communication systems.

The present paper is a direct application of the physical limitations for broadband scattering introduced by Sohl *et al.* (in press, 2007), in which the integrated extinction is related to the long-wavelength polarizability dyadics. The underlying mathematical description is strongly influenced by the consequences of causality and the summation rules and dispersion relations in the scattering theory for the Schrödinger equation (Nussenzveig 1972; Newton 1982; Taylor 1983).

2. Scattering and absorption of antennas

The present theory is inspired by the general scattering formalism of particles and waves by Newton (1982) and Taylor (1983). In fact, based on the assumptions of linearity, time-translational invariance and causality, there is no fundamental difference between antennas and properly modelled scatterers. This kind of fruitful equivalence between antenna and scattering theory has already been encountered in the literature, cf. the limitations on the absorption efficiency by Andersen & Frandsen (2005) and its relation to minimum scattering antennas (MSA). Without loss of generality, the integrated extinction and the theory introduced by Sohl *et al.* (in press) can therefore be argued to also hold for antennas of arbitrary shape. In contrast to the work by Sohl *et al.* (in press), the present paper focuses on the absorption cross-section rather than scattering properties.

For this purpose, consider an antenna of arbitrary shape surrounded by free space and subject to a plane-wave excitation impinging in the $\hat{\boldsymbol{k}}$-direction (figure 1). The antenna is assumed to be lossless with respect to ohmic losses and to satisfy the fundamental principles of linearity, time-translational invariance and causality. The dynamics of the antenna is modelled by the Maxwell equations with general reciprocal anisotropic constitutive relations. The constitutive relations are expressed in terms of the electric and magnetic susceptibility dyadics $\boldsymbol{\chi}_{\mathrm{e}}$ and $\boldsymbol{\chi}_{\mathrm{m}}$, respectively, which model the material properties of the antenna.

The assumption of a lossless antenna is not restrictive since the analysis can be modified to include ohmic losses (see the discussion in §7). In fact, ohmic losses are important for small antennas; when taking such effects into account, this suggests that the lossless antenna is more advantageous than the corresponding antenna with ohmic losses. Recall that $\boldsymbol{\chi}_{\mathrm{e}}$ and $\boldsymbol{\chi}_{\mathrm{m}}$ also depend on the angular frequency ω of the incident plane wave in the presence of losses.

The bounding volume V of the antenna is of arbitrary shape with the restriction that the complete absorption of the incident wave is contained within V. The bounding volume is naturally delimited by a reference plane or a port at which a unique voltage and current relation can be defined (figure 1). The present definition of the antenna structure includes the matching network and is of the same kind as the descriptions by Chu (1948) and Yaghjian & Best (2005). The reflection coefficient Γ at the port is due to the unavoidable impedance mismatch of the antenna over a given wavelength interval (Fano 1950). The present analysis is restricted to single-port antennas with a scalar (single) reflection coefficient. The extension to multiple ports is commented on briefly in §7.

For any antenna, the scattered electric field $\boldsymbol{E}_{\mathrm{s}}$ in the forward direction $\hat{\boldsymbol{k}}$ can be expressed in terms of the forward scattering dyadic $\mathbf{S}$ as (see appendix A)

$$\boldsymbol{E}_{\mathrm{s}}(k, x\hat{\boldsymbol{k}}) = \frac{\mathrm{e}^{\mathrm{i}kx}}{x}\mathbf{S}(k, \hat{\boldsymbol{k}})\cdot\boldsymbol{E}_0 + \mathcal{O}(x^{-2}) \quad \text{as } x\to\infty. \tag{2.1}$$

Here, $\boldsymbol{E}_0$ denotes the Fourier amplitude of the incident field $\boldsymbol{E}_{\mathrm{i}}(\mathrm{c}_0 t - \hat{\boldsymbol{k}}\cdot\boldsymbol{x})$ and k is a complex variable with $\operatorname{Re} k = \omega/\mathrm{c}_0$ and $\operatorname{Im} k \geq 0$. For a large class of antennas, the elements of $\mathbf{S}$ are holomorphic in k and Cauchy's integral theorem can be applied to

$$\varrho(k) = \frac{1}{k^2}\hat{\boldsymbol{p}}_{\mathrm{e}}^{*}\cdot\mathbf{S}(k, \hat{\boldsymbol{k}})\cdot\hat{\boldsymbol{p}}_{\mathrm{e}}, \quad k\in\mathbb{C}. \tag{2.2}$$

Here, $\hat{\boldsymbol{p}}_{\mathrm{e}} = \boldsymbol{E}_0/|\boldsymbol{E}_0|$ denotes the electric polarization, which is assumed to be independent of k.[1] The complex-valued function (2.2) is referred to as the extinction volume, and it provides a holomorphic extension of the extinction cross-section to $\operatorname{Im} k \geq 0$ (see appendix A).

A dispersion relation or summation rule for the extinction cross-section can be derived in terms of the electric and magnetic polarizability dyadics $\boldsymbol{\gamma}_{\mathrm{e}}$ and $\boldsymbol{\gamma}_{\mathrm{m}}$, respectively. The derivation is based on energy conservation via the optical theorem by Newton (1982) and Taylor (1983). The optical theorem $\sigma_{\mathrm{ext}} = 4\pi k \operatorname{Im}\varrho$ and the asymptotic behaviour of the extinction volume ϱ in the long-wavelength limit, $|k|\to 0$, are the key building blocks in the derivation. The result is the integrated extinction

$$\int_0^\infty \sigma_{\mathrm{ext}}(\lambda)\mathrm{d}\lambda = \pi^2(\hat{\boldsymbol{p}}_{\mathrm{e}}^{*}\cdot\boldsymbol{\gamma}_{\mathrm{e}}\cdot\hat{\boldsymbol{p}}_{\mathrm{e}} + \hat{\boldsymbol{p}}_{\mathrm{m}}^{*}\cdot\boldsymbol{\gamma}_{\mathrm{m}}\cdot\hat{\boldsymbol{p}}_{\mathrm{m}}), \tag{2.3}$$

where the magnetic (or cross) polarization $\hat{\boldsymbol{p}}_{\mathrm{m}} = \hat{\boldsymbol{k}}\times\hat{\boldsymbol{p}}_{\mathrm{e}}$ has been introduced. The functional dependence on $\hat{\boldsymbol{k}}$ and $\hat{\boldsymbol{p}}_{\mathrm{e}}$ is, for simplicity, suppressed from the argument on the l.h.s. of (2.3). Note that (2.3) can also be formulated in $k = 2\pi/\lambda$ via the transformation $\sigma_{\mathrm{ext}}(\lambda)\to 2\pi\sigma_{\mathrm{ext}}(2\pi/k)/k^2$. For details on the derivation of (2.3) and definition of the extinction cross-section σ_{ext} and the polarizability dyadics $\boldsymbol{\gamma}_{\mathrm{e}}$ and $\boldsymbol{\gamma}_{\mathrm{m}}$, see appendices A and B. The integrated extinction applied to scattering problems is exploited by Sohl *et al.* (in press).

[1] Observe that the assumption that $\hat{\boldsymbol{p}}_{\mathrm{e}}$ is independent of k does not imply that the polarization of the antenna in figure 1 is frequency independent.

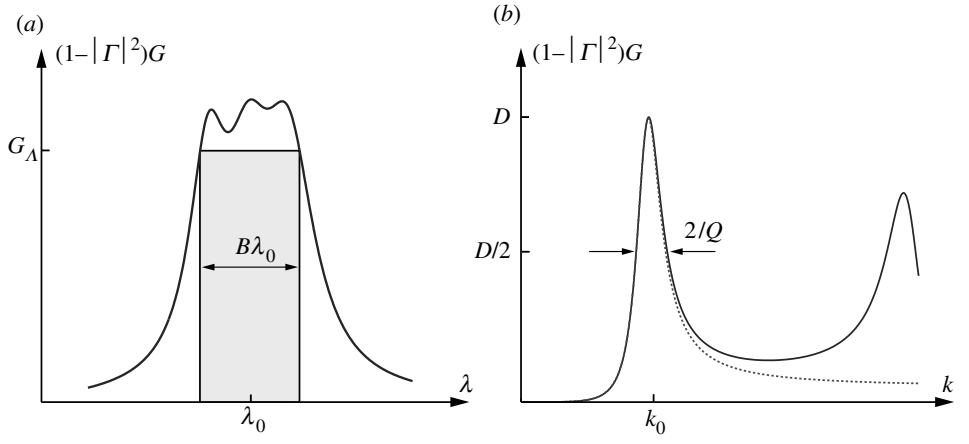

Figure 2. Illustration of the two types of physical limitations considered in this paper: (*a*) $G_A B$ represented by the shaded box and (*b*) D/Q related to the dotted resonance model.

It is important to note at this point that the r.h.s. of (2.3) depends only on the long-wavelength limit or static response of the antenna, whereas the l.h.s. is a dynamic quantity which includes the absorption and scattering properties of the antenna. Furthermore, electric and magnetic properties are seen to be treated on equal footing in (2.3), in terms of both material properties and polarization description.

The antenna parameters of importance in this paper are the partial gain G and the partial directivity D (IEEE 1993; Gustafsson *et al.* 2007). In general, both G and D depend on the incident direction $\hat{\boldsymbol{k}}$ and the electric polarization $\hat{\boldsymbol{p}}_{\mathrm{e}}$ as well as the wavenumber k. In addition, the partial realized gain, $(1-|\Gamma|^2)G$, depends on the reflection coefficient Γ. In the forthcoming analysis, the relative bandwidth B, the Q-factor and the associated centre wavelength λ_0 are naturally introduced as intrinsic parameters in the sense that neither of them depends on $\hat{\boldsymbol{k}}$ or $\hat{\boldsymbol{p}}_{\mathrm{e}}$ for a given single-port antenna.

Two different types of bounds on the first resonance of an antenna are addressed in this paper (figure 2). The bounds relate the integral (2.3) of two generic integrands to the polarizability dyadics. The bound on the partial realized gain, $(1-|\Gamma|^2)G$, in figure 2*a* takes the form of a box, i.e. it estimates the integral with the bandwidth multiplied by the partial realized gain. The bound in figure 2*b* uses the classical resonance shape of the integrand giving a bound expressed in terms of the partial directivity and the associated Q-factor.

3. Limitations on bandwidth and gain

From the definition of the extinction cross-section σ_{ext}, it is clear that it is non-negative and bounded from below by the absorption cross-section σ_{a}. For an unmatched antenna, σ_{a} is reduced by the reflection loss $1-|\Gamma|^2$ according to $\sigma_{\mathrm{a}}=(1-|\Gamma|^2)\sigma_{\mathrm{a0}}$, where σ_{a0} denotes the absorption cross-section or partial effective area for the corresponding perfectly matched antenna by Silver (1949) and IEEE (1993). The absorption cross-section σ_{a0} is by reciprocity related to the partial antenna directivity D as $D=4\pi\sigma_{\mathrm{a0}}/\lambda^2$ (Silver 1949). Thus, for any

wavelength $\lambda \in [0, \infty)$,

$$\sigma_{\mathrm{ext}} \geq \sigma_{\mathrm{a}} = (1-|\Gamma|^2)\sigma_{\mathrm{a0}} = \frac{1}{4\pi}(1-|\Gamma|^2)\lambda^2 D. \tag{3.1}$$

Recall that D depends on the electric polarization $\hat{\boldsymbol{p}}_{\mathrm{e}}$ as well as the incident direction $\hat{\boldsymbol{k}}$. In the present case of no ohmic losses, the partial gain G coincides with the partial directivity D.

Introduce the wavelength interval $\Lambda = [\lambda_1, \lambda_2]$ with centre wavelength $\lambda_0 = (\lambda_1 + \lambda_2)/2$ and associated relative bandwidth

$$B = 2\frac{\lambda_2 - \lambda_1}{\lambda_2 + \lambda_1} = 2\frac{k_1 - k_2}{k_2 + k_1},$$

where $0 < B \leq 2$ and $k = 2\pi/\lambda \in K$ denotes the angular wavenumber in $K = [k_2, k_1]$. Thus, for any wavelength interval Λ, the estimate $\sigma_{\mathrm{ext}} \geq \sigma_{\mathrm{a}}$ in (3.1) yields

$$\int_0^\infty \sigma_{\mathrm{ext}}(\lambda)\mathrm{d}\lambda \geq \int_\Lambda \sigma_{\mathrm{a}}(\lambda)\mathrm{d}\lambda = \frac{1}{4\pi}\int_\Lambda (1-|\Gamma|^2)\lambda^2 G(\lambda)\mathrm{d}\lambda, \tag{3.2}$$

where $D = G$ is used.[2]

In order to simplify the notation, introduce $G_\Lambda = \inf_{\lambda\in\Lambda}(1-|\Gamma|^2)G$ as the minimum partial realized gain over the wavelength interval Λ. Following this notation, the integral on the r.h.s. of (3.2) can be estimated from below as

$$\int_\Lambda (1-|\Gamma|^2)\lambda^2 G(\lambda)\mathrm{d}\lambda \geq G_\Lambda \int_\Lambda \lambda^2 \mathrm{d}\lambda = \lambda_0^3 G_\Lambda B\left(1 + \frac{B^2}{12}\right). \tag{3.3}$$

Without loss of generality, the factor $1 + B^2/12$ can be estimated from below by unity. This estimate is also supported by the fact that $B \ll 2$ in many applications. Based upon this observation, (2.3), (3.2) and (3.3) can be summarized to yield the following limitation on the product $G_\Lambda B$ valid for any antenna satisfying the general assumptions stated in §2:

$$G_\Lambda B \leq \frac{4\pi^3}{\lambda_0^3}(\hat{\boldsymbol{p}}_{\mathrm{e}}^* \cdot \boldsymbol{\gamma}_{\mathrm{e}} \cdot \hat{\boldsymbol{p}}_{\mathrm{e}} + \hat{\boldsymbol{p}}_{\mathrm{m}}^* \cdot \boldsymbol{\gamma}_{\mathrm{m}} \cdot \hat{\boldsymbol{p}}_{\mathrm{m}}). \tag{3.4}$$

Relation (3.4) is one of the main results of this paper. Note that the factor $4\pi^3/\lambda_0^3$ can be neatly expressed as $k_0^3/2$ in terms of the angular wavenumber $k_0 = 2\pi/\lambda_0$.

The estimate $1 + B^2/12 \geq 1$ in (3.3) is motivated by the simple form of (3.4). In broadband applications, B in general is not small compared with unity, and the higher order term in B should be included on the l.h.s. of (3.4).

The r.h.s. of (3.4) depends on both $\hat{\boldsymbol{p}}_{\mathrm{e}}$ and $\hat{\boldsymbol{k}} = \hat{\boldsymbol{p}}_{\mathrm{e}} \times \hat{\boldsymbol{p}}_{\mathrm{m}}$, as well as the long-wavelength limit (static limit with respect to $k = 2\pi/\lambda$) material properties and shape of the antenna. It is indeed surprising that it is just the long-wavelength limit properties of the antenna that bound the product $G_\Lambda B$ in (3.4). Since $\boldsymbol{\gamma}_{\mathrm{e}}$ and $\boldsymbol{\gamma}_{\mathrm{m}}$ are proportional to the volume V of the antenna, by Sohl *et al.* (in press), it follows from (3.4) that the upper bound on the product $G_\Lambda B$ is directly proportional to V/λ_0^3 or $k_0^3 a^3$, where a denotes the radius of the volume-equivalent sphere.

[2] The equality sign on the left hand side in (3.2) is motivated by the broadband absorption efficiency introduced in (3.7).

In many antenna applications, it is desirable to bound the product $G_A B$ independently of the material properties. For this purpose, we introduce the high-contrast polarizability dyadic $\boldsymbol{\gamma}_\infty$ as the limit of either $\boldsymbol{\gamma}_\mathrm{e}$ or $\boldsymbol{\gamma}_\mathrm{m}$ when the elements of $\boldsymbol{\chi}_\mathrm{e}$ or $\boldsymbol{\chi}_\mathrm{m}$ in the long-wavelength limit simultaneously approach infinity.[3] Note that this definition implies that $\boldsymbol{\gamma}_\infty$ is independent of any material properties, depending only on the geometry of the antenna. From the variational properties of $\boldsymbol{\gamma}_\mathrm{e}$ and $\boldsymbol{\gamma}_\mathrm{m}$ discussed by Sohl *et al.* (in press) and references therein, it follows that both $\boldsymbol{\gamma}_\mathrm{e}$ and $\boldsymbol{\gamma}_\mathrm{m}$ are bounded from above by $\boldsymbol{\gamma}_\infty$. Hence, (3.4) yields

$$G_A B \leq \frac{4\pi^3}{\lambda_0^3}(\hat{\boldsymbol{p}}_\mathrm{e}^* \cdot \boldsymbol{\gamma}_\infty \cdot \hat{\boldsymbol{p}}_\mathrm{e} + \hat{\boldsymbol{p}}_\mathrm{m}^* \cdot \boldsymbol{\gamma}_\infty \cdot \hat{\boldsymbol{p}}_\mathrm{m}). \tag{3.5}$$

The introduction of the high-contrast polarizability dyadic $\boldsymbol{\gamma}_\infty$ in (3.5) is the starting point of the analysis below.

The high-contrast polarizability dyadic $\boldsymbol{\gamma}_\infty$ is real-valued and symmetric, and consequently diagonalizable with real-valued eigenvalues. Let $\gamma_1 \geq \gamma_2 \geq \gamma_3$ denote the three eigenvalues. Based on the constraint $\hat{\boldsymbol{p}}_\mathrm{e} \cdot \hat{\boldsymbol{p}}_\mathrm{m} = 0$, which is a consequence of the free space plane-wave excitation, the r.h.s. of (3.5) can be estimated from above as

$$\sup_{\hat{\boldsymbol{p}}_\mathrm{e} \cdot \hat{\boldsymbol{p}}_\mathrm{m} = 0} G_A B \leq \frac{4\pi^3}{\lambda_0^3}(\gamma_1 + \gamma_2). \tag{3.6}$$

The interpretation of the operator $\sup_{\hat{\boldsymbol{p}}_\mathrm{e} \cdot \hat{\boldsymbol{p}}_\mathrm{m} = 0}$ is polarization matching, i.e. the polarization of the antenna coincides with the polarization of the incident wave. In the case of non-magnetic antennas, $\boldsymbol{\gamma}_\mathrm{m} = \mathbf{0}$, the second eigenvalue γ_2 in (3.6) vanishes. Hence, the r.h.s. of (3.6) can be improved by at most a factor of 2 by using magnetic materials. Note that the upper bounds in (3.5) and (3.6) coincide when $\boldsymbol{\gamma}_\infty$ is isotropic.

Since γ_1 and γ_2 depend only on the long-wavelength properties of the antenna, they can easily be calculated for arbitrary geometries using either the finite element method (FEM) or the method of moments (MoM). Numerical results of γ_1 and γ_2 for the Platonic solids, the rectangular parallelepiped and some classical antennas are presented by Gustafsson *et al.* (2007). The influence of supporting ground planes and the validity of the method of images for high-contrast polarizability calculations are presented by Gustafsson *et al.* (2007).

The estimate in (3.2) can be improved based on *a priori* knowledge of the scattering properties of the antenna. In fact, $\sigma_\mathrm{ext} \geq \sigma_\mathrm{a}$ in (3.1) may be replaced by $\sigma_\mathrm{ext} = \sigma_\mathrm{a}/\eta$, where $0 < \eta \leq 1$ denotes the absorption efficiency of the antenna (Andersen & Frandsen 2005). For most antennas at the resonance frequency, $\eta \leq 1/2$, but exceptions to this rule of thumb exist. In particular, MSA defined by $\eta = 1/2$ yield an additional factor of 2 on the r.h.s. of (3.1). The inequality in (3.2) can be replaced by the equality

$$\int_A \sigma_\mathrm{ext}(\lambda)\mathrm{d}\lambda = \bar{\eta}^{-1} \int_A \sigma_\mathrm{a}(\lambda)\mathrm{d}\lambda. \tag{3.7}$$

[3] Recall that $\boldsymbol{\chi}_\mathrm{e}$ and $\boldsymbol{\chi}_\mathrm{m}$ are real-valued in the long-wavelength limit. In the case of finite or infinite conductivity, see Gustafsson *et al.* (2007).

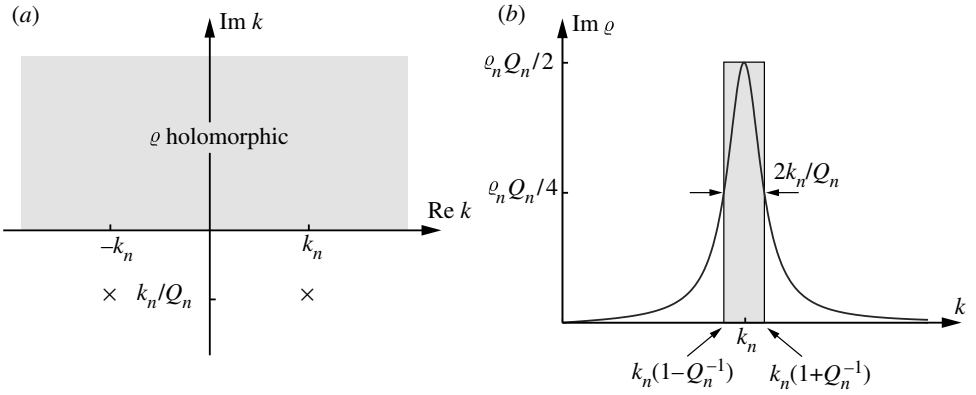

Figure 3. (*a*) The symmetrically distributed pair of poles (cross) of the extinction volume ϱ in the complex k-plane and (*b*) the corresponding single resonance model of Im ϱ when $Q_n \gg 1$.

The constant $\bar{\eta}$ is bounded from above by the absorption efficiency via $\bar{\eta} \leq \sup_{\lambda \in \Lambda} \eta$ and provides a broadband generalization of the absorption efficiency. If $\bar{\eta}$ is invoked in (3.2), the r.h.s. of the inequalities (3.4), (3.5) and (3.6) are sharpened by the multiplicative factor $\bar{\eta}$.

4. Limitations on *Q*-factor and directivity

Under the assumption of N non-interfering resonances characterized by the real-valued angular wavenumbers k_n, a multiple resonance model for the absorption cross-section is

$$\sigma_{\mathrm{a}}(k) = 2\pi \sum_{n=1}^{N} \varrho_n \frac{Q_n k_n}{1 + Q_n^2 (k/k_n - k_n/k)^2/4}, \tag{4.1}$$

where k is assumed to be real-valued and ϱ_n are positive weight functions satisfying $\sum_n \varrho_n = \varrho(0)$. Here, the Q-factor of the resonance at k_n is denoted by Q_n, and, for $Q_n \gg 1$, the associated relative half-power bandwidth is $B_n \sim 2/Q_n$ (figure 3). Recall that $Q_n \geq 1$ is consistent with $0 < B_n \leq 2$. For the resonance model (4.1), one can argue that Q_n in fact coincides with the corresponding antenna Q-factor by Gustafsson *et al.* (2007) when the relative bandwidth $2/Q_n$ is based on the half-power threshold (Yaghjian & Best 2005; Gustafsson & Nordebo 2006). In the case of strongly interfering resonances, either the model (4.1) has to be modified or the estimates in §3 have to be used.

The absorption cross-section is the imaginary part, $\sigma_{\mathrm{a}} = 4\pi k \,\mathrm{Im}\, \varrho_{\mathrm{a}}$, of the function

$$\varrho_{\mathrm{a}}(k) = \sum_{n=1}^{N} \varrho_n \frac{\mathrm{i} Q_n k_n/(2k)}{1 - \mathrm{i} Q_n (k/k_n - k_n/k)/2}, \tag{4.2}$$

for real-valued k. The function $\varrho_{\mathrm{a}}(k)$ is holomorphic for $\mathrm{Im}\, k > 0$ and has a symmetrically distributed pair of poles for $\mathrm{Im}\, k < 0$ (figure 3). The integrated

absorption cross-section is

$$\frac{1}{4\pi^2}\int_{-\infty}^{\infty}\frac{\sigma_{\mathrm{a}}(k)}{k^2}\,\mathrm{d}k=\varrho_{\mathrm{a}}(0)=\bar{\eta}\varrho(0)\leq\varrho(0), \tag{4.3}$$

where $\varrho(0)$ is given by the long-wavelength limit (A 4).

For antennas with a dominant first resonance at $k=k_1$, it follows from (3.1) and (4.1) that the partial realized gain satisfies

$$(1-|\Gamma|^2)G=\frac{k^2\sigma_{\mathrm{a}}}{\pi}\leq\varrho(0)\frac{2k^2Qk_1}{1+Q^2(k/k_1-k_1/k)^2/4}, \tag{4.4}$$

where $\varrho_1\leq\varrho(0)$ has been used. The r.h.s. of (4.4) reaches its maximum value $\varrho(0)2k_1^3Q/(1-Q^{-2})$ at $k_0=k_1(1-2Q^{-2})^{-1/2}$ or $k_0=k_1+\mathcal{O}(Q^{-2})$ as $Q\to\infty$. Hence, k_0 is a good approximation to k_1 if $Q\gg1$. For a lossless antenna, which is perfectly matched at $k=k_0$, the partial realized gain $(1-|\Gamma|^2)G$ coincides with the partial directivity D. Under this assumption, (4.4) yields $D/Q\leq\varrho(0)2k_1^3/(1-Q^{-2})$ which can be further estimated from above as

$$\frac{D}{Q}\leq\frac{k_0^3}{2\pi}(\hat{\boldsymbol{p}}_{\mathrm{e}}^{*}\cdot\boldsymbol{\gamma}_{\mathrm{e}}\cdot\hat{\boldsymbol{p}}_{\mathrm{e}}+\hat{\boldsymbol{p}}_{\mathrm{m}}^{*}\cdot\boldsymbol{\gamma}_{\mathrm{m}}\cdot\hat{\boldsymbol{p}}_{\mathrm{m}}), \tag{4.5}$$

where (A 4) has been used. Relations (4.5) and (3.4) constitute the main results of this paper. Analogous to (3.5) and (3.6), it is clear that (4.5) can be estimated from above by the high-contrast polarizability dyadic $\boldsymbol{\gamma}_\infty$ and the associated eigenvalues γ_1 and γ_2, namely

$$\sup_{\hat{\boldsymbol{p}}_{\mathrm{e}}\cdot\hat{\boldsymbol{p}}_{\mathrm{m}}=0}\frac{D}{Q}\leq\frac{k_0^3}{2\pi}(\gamma_1+\gamma_2). \tag{4.6}$$

Here, (4.6) is subject to polarization matching and therefore independent of the electric and magnetic polarizations $\hat{\boldsymbol{p}}_{\mathrm{e}}$ and $\hat{\boldsymbol{p}}_{\mathrm{m}}$, respectively. Note that the upper bounds in (4.5) and (4.6) differ from the corresponding results in (3.4) and (3.6) only by a factor of π, i.e. $G_{\mathcal{A}}B\leq\pi C$ and $D/Q\leq C$. Hence, it is sufficient to consider either the $G_{\mathcal{A}}B$ or the D/Q bound for a specific antenna. The estimates (4.5) and (4.6) can be improved by the multiplicative factor $\bar{\eta}$ if *a priori* knowledge of the scattering properties of the antenna (3.7) is invoked in (4.4).

The resonance model for the absorption cross-section in (4.1) is also directly applicable to the theory of broadband scattering (Sohl *et al.* in press). In that reference, (4.1) can be used to model absorption and scattering properties and yield new limitations on broadband scattering.

5. Comparison with Chu and Chu–Fano

In this section, the bounds on $G_{\mathcal{A}}B$ and D/Q subject to matched polarizations, i.e. inequalities (3.6) and (4.6), are compared with the corresponding results by Chu and Fano (Chu 1948; Fano 1950).

(*a*) *Limitations on* Q*-factor and directivity*

The classical limitations derived by Chu (1948) relate the Q-factor and the directivity D to the quantity $k_0 a$ of the smallest circumscribing sphere. Using the notation of §§3 and 4, the classical result by Chu for an omni-directional antenna (for example in the azimuth plane) reads

$$\sup_{\hat{\boldsymbol{p}}_{\mathrm{e}}\cdot\hat{\boldsymbol{p}}_{\mathrm{m}}=0}\frac{D}{Q}\leq\frac{3}{2}\frac{k_0^3a^3}{k_0^2a^2+1}=\frac{3}{2}k_0^3a^3+\mathcal{O}(k_0^5a^5)\quad\text{as}\quad k_0a\to 0. \tag{5.1}$$

In the general case of both TE- and TM-modes, (5.1) must be modified (see Hansen 2006), namely

$$\sup_{\hat{\boldsymbol{p}}_{\mathrm{e}}\cdot\hat{\boldsymbol{p}}_{\mathrm{m}}=0}\frac{D}{Q}\leq\frac{6k_0^3a^3}{2k_0^2a^2+1}=6k_0^3a^3+\mathcal{O}(k_0^5a^5)\quad\text{as}\quad k_0a\to 0. \tag{5.2}$$

Note that (5.2) differs from (5.1) by approximately a factor of 4 when $k_0 a \ll 1$.

The bounds in (5.1) and (5.2) should be compared with the corresponding result in §4 for the sphere. For a sphere of radius a, the eigenvalues γ_1 and γ_2 are degenerated and equal to $4\pi a^3$, see §6. Insertion of $\gamma_1=\gamma_2=4\pi a^3$ into (4.6) yields $\sup_{\hat{\boldsymbol{p}}_{\mathrm{e}}\cdot\hat{\boldsymbol{p}}_{\mathrm{m}}=0} D/Q\leq C$, where the constant C is given by

$$C=4k_0^3a^3,\qquad C=2k_0^3a^3,\qquad C=k_0^3a^3. \tag{5.3}$$

The three different cases in (5.3) correspond to both electric and magnetic material properties ($C=4k_0^3a^3$), pure electric material properties ($C=2k_0^3a^3$) and pure electric material properties with *a priori* knowledge of minimum scattering characteristics ($C=k_0^3a^3$ with $\bar{\eta}=1/2$). Note that the third case in (5.3) can be generally expressed as $C=2k_0^3a^3\bar{\eta}$ for any broadband absorption efficiency $0<\bar{\eta}\leq 1$. The bounds in (5.2) and (5.3) are comparable although the new limitations (5.3) are sharper. In the omnidirectional case, (5.1) provides a sharper bound than (5.3), except for the pure electric case with absorption efficiency $\bar{\eta}<3/4$.

(*b*) *Limitations on bandwidth and gain*

The limitation (3.6) should also be compared with the result of Chu when the Fano theory of broadband matching is used. The Fano theory includes the impedance variation over the frequency interval to yield limitations on the bandwidth (see Fano (1950)). For a resonance circuit model, the Fano theory yields that the relation between B and Q is (Gustafsson & Nordebo 2006)

$$B\leq\frac{\pi}{Q\ln 1/|\Gamma|}. \tag{5.4}$$

The reflection coefficient Γ is due to the mismatch of the antenna. It is related to the standing wave ratio (SWR) as $|\Gamma|=(\mathrm{SWR}-1)/(1+\mathrm{SWR})$.

Introduce Q_{s} as the Q-factor of the smallest circumscribing sphere with $1/Q_{\mathrm{s}}=k_0^3a^3+\mathcal{O}(k_0^5a^5)$ as $k_0a\to 0$ for omnidirectional antennas. Under this assumption, it follows from (5.1) that $\sup_{\hat{\boldsymbol{p}}_{\mathrm{e}}\cdot\hat{\boldsymbol{p}}_{\mathrm{m}}=0} D\leq 3Q/2Q_{\mathrm{s}}$. Insertion of this inequality into

(5.4) then yields

$$\sup_{\hat{\boldsymbol{p}}_e\cdot\hat{\boldsymbol{p}}_m=0} G_A B \le \frac{3\pi}{2}\,\frac{1-|\Gamma|^2}{\ln 1/|\Gamma|}\,k_0^3 a^3. \tag{5.5}$$

For a given $k_0 a$, the r.h.s. of (5.5) is monotone in $|\Gamma|$ and bounded from above by $3\pi k_0^3 a^3$. However, note that the Chu–Fano limitation (5.5) is restricted to omnidirectional antennas with $k_0 a \ll 1$.

Inequality (5.5) should be compared with the corresponding result in §3 for the smallest circumscribing sphere. Since the upper bounds (3.6) and (4.6) differ only by a factor of π, i.e. $\sup_{\hat{\boldsymbol{p}}_e\cdot\hat{\boldsymbol{p}}_m=0} G_A B \le C'$ and $\sup_{\hat{\boldsymbol{p}}_e\cdot\hat{\boldsymbol{p}}_m=0} D/Q \le C$ where $C'=\pi C$, it follows from (5.3) that

$$C' = 4\pi k_0^3 a^3, \qquad C' = 2\pi k_0^3 a^3, \qquad C' = \pi k_0^3 a^3. \tag{5.6}$$

The three cases in (5.3) correspond to both electric and magnetic material properties ($C'=4\pi k_0^3 a^3$), pure electric material properties ($C'=2\pi k_0^3 a^3$) and pure electric material properties with *a priori* knowledge of minimum scattering characteristics ($C'=\pi k_0^3 a^3$).

The limitations on $G_A B$ based on (5.6) are comparable with (5.5) for most reflection coefficients $|\Gamma|$. For $|\Gamma|<0.65$ the Chu–Fano limitation (5.5) provides a slightly sharper bound on $G_A B$ than (5.6) for pure electric materials. However, recall that the spherical geometry gives an unfavourable comparison with the present theory, since for many antennas the eigenvalues γ_1 and γ_2 are reduced considerably compared with the smallest circumscribing sphere, cf. the dipole and loop antennas (Gustafsson *et al.* 2007).

6. Ellipsoidal geometries

Closed-form expressions of $\boldsymbol{\gamma}_e$ and $\boldsymbol{\gamma}_m$ exist for the ellipsoidal geometries (Sohl *et al.* in press), namely

$$\boldsymbol{\gamma}_e = V\boldsymbol{\chi}_e\cdot(\mathbf{I}+\mathbf{L}\cdot\boldsymbol{\chi}_e)^{-1}, \qquad \boldsymbol{\gamma}_m = V\boldsymbol{\chi}_m\cdot(\mathbf{I}+\mathbf{L}\cdot\boldsymbol{\chi}_m)^{-1}. \tag{6.1}$$

Here, $\mathbf{I}$ denotes the unit dyadic and $V=4\pi a_1 a_2 a_3/3$ is the volume of the ellipsoid in terms of the semi-axes a_j. The depolarizability dyadic $\mathbf{L}$ is real-valued and symmetric, and hence diagonalizable with real-valued eigenvalues. The eigenvalues of $\mathbf{L}$ are the depolarizing factors L_j given by

$$L_j = \frac{a_1 a_2 a_3}{2}\int_0^\infty \frac{\mathrm{d}s}{(s+a_j^2)\sqrt{(s+a_1^2)(s+a_2^2)(s+a_3^2)}}, \quad j=1,2,3. \tag{6.2}$$

The depolarizing factors L_j satisfy $0\le L_j\le 1$ and $\sum_j L_j = 1$. The semi-axes a_j are assumed to be ordered such that $L_1\le L_2\le L_3$. Closed-form expressions of (6.2) in terms of the semi-axis ratio $\xi=(\min_j a_j)/(\max_j a_j)$ exist for the ellipsoids of revolution, i.e. the prolate spheroids ($L_2=L_3$) and the oblate spheroids ($L_1=L_2$), see appendix C.

The high-contrast polarizability dyadic $\boldsymbol{\gamma}_\infty$ is given by (6.1) as the elements of $\boldsymbol{\chi}_e$ or $\boldsymbol{\chi}_m$ simultaneously approach infinity. From (6.1) it is clear that the eigenvalues of $\boldsymbol{\gamma}_\infty$ are given by $\gamma_j = V/L_j$. For the prolate and oblate spheroids, V is neatly expressed in terms of the volume $V_s=4\pi a^3/3$ of the smallest

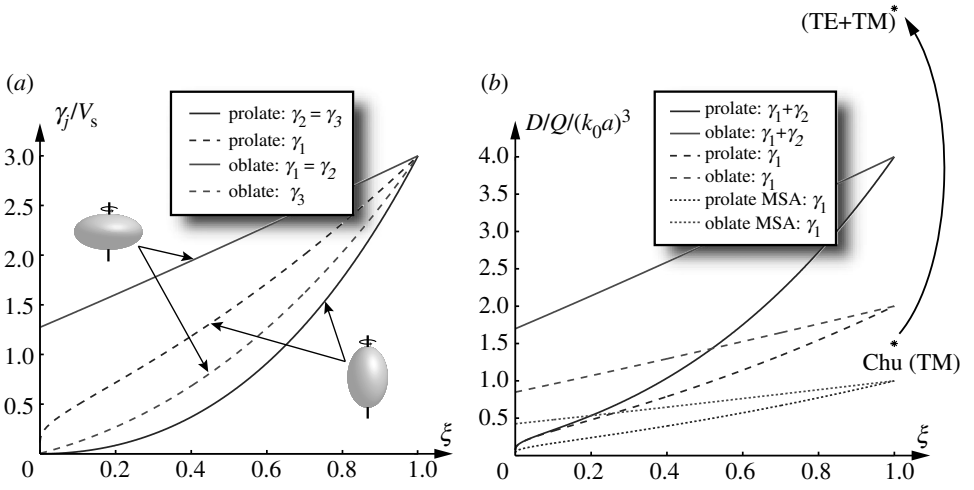

Figure 4. (*a*) The eigenvalues $\gamma_1 \geq \gamma_2 \geq \gamma_3$ and (*b*) the quotient D/Q for the prolate and oblate spheroids as functions of the semi-axis ratio ξ. Note the normalization with the volume $V_s = 4\pi a^3/3$ of the smallest circumscribing sphere.

circumscribing sphere. The results are $V = \xi^2 V_s$ and $V = \xi V_s$ for the prolate and oblate spheroids, respectively. The eigenvalues γ_1 and γ_2 for the prolate and oblate spheroids are depicted in figure 4*a*. Note that the curves for the oblate spheroid approach $4/\pi$ in the limit as $\xi \to 0$, see appendix C. The corresponding limiting value for the curves as $\xi \to 1$ is 3.

The general bound on $G_A B$ for arbitrary ellipsoidal geometries is obtained by inserting (6.1) into (3.4), i.e.

$$G_A B \leq \frac{4\pi^3 V}{\lambda_0^3} (\hat{\boldsymbol{p}}_e^* \cdot \boldsymbol{\chi}_e \cdot (\mathbf{I} + \mathbf{L} \cdot \boldsymbol{\chi}_e)^{-1} \cdot \hat{\boldsymbol{p}}_e + \hat{\boldsymbol{p}}_m^* \cdot \boldsymbol{\chi}_m \cdot (\mathbf{I} + \mathbf{L} \cdot \boldsymbol{\chi}_m)^{-1} \cdot \hat{\boldsymbol{p}}_m). \tag{6.3}$$

Independent of both material properties and polarization effects, the r.h.s. of (6.3) can be estimated from above in analogy with (3.6). The result is

$$\sup_{\hat{\boldsymbol{p}}_e \cdot \hat{\boldsymbol{p}}_m = 0} G_A B \leq \frac{4\pi^3 V}{\lambda_0^3} \left(\frac{1}{L_1} + \frac{1}{L_2} \right). \tag{6.4}$$

In the non-magnetic case, the second term on the r.h.s. of (6.3) and (6.4) vanishes. For the prolate and oblate spheroids, the closed-form expressions of L_j in appendix C can be introduced to yield explicit upper bounds on $G_A B$.

The corresponding results for the quotient D/Q are obtained from the observation that $G_A B \leq \pi C$ is equivalent to $D/Q \leq C$, see §4. For the general case including polarization and material properties, (6.3) yields

$$\frac{D}{Q} \leq \frac{k_0^3 V}{2\pi} (\hat{\boldsymbol{p}}_e^* \cdot \boldsymbol{\chi}_e \cdot (\mathbf{I} + \mathbf{L} \cdot \boldsymbol{\chi}_e)^{-1} \cdot \hat{\boldsymbol{p}}_e + \hat{\boldsymbol{p}}_m^* \cdot \boldsymbol{\chi}_m \cdot (\mathbf{I} + \mathbf{L} \cdot \boldsymbol{\chi}_m)^{-1} \cdot \hat{\boldsymbol{p}}_m). \tag{6.5}$$

Analogous to (6.4), the restriction to matched polarizations for the quotient D/Q reads

$$\sup_{\hat{\boldsymbol{p}}_e \cdot \hat{\boldsymbol{p}}_m = 0} \frac{D}{Q} \leq \frac{k_0^3 V}{2\pi} \left(\frac{1}{L_1} + \frac{1}{L_2} \right). \tag{6.6}$$

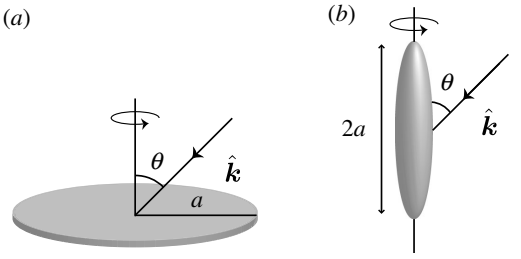

Figure 5. Geometry of the (*a*) circular disc and (*b*) needle.

The upper bound in (6.6) is depicted in figure 4*b* for the prolate and oblate spheroids. The solid curves correspond to combined electric and magnetic material properties, while the dashed curves represent the pure electric case. The non-magnetic minimum scattering case ($\bar{\eta}=1/2$) is given by the dotted curves. Note that the three curves in figure 4*b* vanish for the prolate spheroid as $\xi\to 0$. The corresponding limiting values for the oblate spheroid are $16/3\pi$, $8/3\pi$ and $4/3\pi$, see appendix C.

The curves depicted in figure 4*b* should be compared with the classical results for the sphere in (5.1) and (5.2). The omnidirectional bound (5.1) and its generalization (5.2) are marked in figure 4 by Chu (TE) and (TE+TM), respectively. From figure 4, it is clear that (6.6) provides a sharper bound than (5.2). For omnidirectional antennas, (5.1) is slightly sharper than (6.6) for the sphere, but when *a priori* knowledge of minimum scattering characteristics ($\bar{\eta}=1/2$) is used, the reverse conclusion holds. Recall that the classical results in §5*a* are restricted to the sphere, in contrast to the theory introduced in this paper.

Based on the results in appendix C, it is interesting to evaluate (6.4) in the limit as $\xi\to 0$. This limit corresponds to the axially symmetric needle and circular disc in figure 5. For a needle of length $2a$ with semi-axis ratio $\xi\ll 1$, (C 3) inserted into (6.4) yields

$$G_A B \le \frac{16\pi^4 a^3}{3\lambda_0^3}\,\frac{f(\theta)}{\ln 2/\xi - 1} + \mathcal{O}(\xi^2) \quad \text{as} \quad \xi\to 0. \tag{6.7}$$

Here, $f(\theta)=\sin^2\theta$ for the TE- and TM-polarizations in the case of both electric and magnetic material properties. In the non-magnetic case, $f(\theta)=0$ for the TE- and $f(\theta)=\sin^2\theta$ for the TM-polarization. Note that the $\sin^2\theta$ term in (6.7) and the logarithmic singularity in the denominator agree with the radiation pattern and the impedance of the dipole antenna by Elliott (2003) and Gustafsson *et al.* (2007).

The corresponding result for the circular disc of radius a is non-vanishing in the limit as $\xi\to 0$, namely

$$G_A B \le \frac{64\pi^3 a^3}{3\lambda_0^3} f(\theta). \tag{6.8}$$

Here, $f(\theta)=1+\cos^2\theta$ for the TE- and TM-polarizations in the case of both electric and magnetic material properties. In the non-magnetic case, $f(\theta)=1$ for the TE- and $f(\theta)=\cos^2\theta$ for the TE polarization. Note the direct application of (6.8) for planar spiral antennas.

7. Conclusion and future work

In this paper, physical limitations on reciprocal antennas of arbitrary shape are derived based on the holomorphic properties of the forward scattering dyadic. The results are very general in the sense that the underlying analysis solely depends on energy conservation and the fundamental principles of linearity, time-translational invariance and causality. Several deficiencies and drawbacks of the classical limitations of Chu and Wheeler (Wheeler 1947; Chu 1948) are overcome with this new formulation. The main advantages of the new limitations are at least fivefold: (i) they hold for arbitrary antenna geometries, (ii) they are formulated in the gain and bandwidth as well as the directivity and the Q-factor, (iii) they permit the study of polarization effects such as diversity in applications for MIMO communication systems, (iv) they successfully separate electric and magnetic antenna properties in terms of the intrinsic material parameters, and (v) they are isoperimetric from a practical point of view in the sense that, for some geometries, physical antennas can be realized which yield equality in the limitations.

The main results of the present theory are the limitations on the partial realized gain and partial directivity in (3.4) and (4.5), respectively. Since the upper bounds in (3.4) and (4.5) are proportional to $k_0^3 a^3$, where a denotes the radius of, say, the volume equivalent sphere, it is clear that no broadband electrically small antennas exist unless gain or directivity is sacrificed for bandwidth or Q-factor. This is also the main conclusion by Hansen (2006), which is presented on more vague grounds. Furthermore, the present theory suggests that, in addition to electric material properties, magnetic materials could also be invoked in the antenna design to increase the performance, cf. the ferrite-loaded loop antenna by Elliott (2003).

In contrast to the classical results by Chu and Wheeler (Wheeler 1947; Chu 1948), these new limitations are believed to be isoperimetric in the sense that the bounds hold for some physical antenna. A striking example of the intrinsic accuracy of the theory is illustrated by the dipole antenna by Gustafsson *et al.* (2007). In fact, many wire antennas are believed to be close to the upper bounds since these antennas make effective use of their volumes.

It is important to remember that *a priori* knowledge of the absorption efficiency $\eta = \sigma_{\mathrm{a}}/\sigma_{\mathrm{ext}}$ can sharpen the bounds in (3.4) and (4.5), cf. the dipole antenna by Gustafsson *et al.* (2007) for which $\bar{\eta} \approx 1/2$ is used. Similarly, *a priori* knowledge of the radiation efficiency, η_{r}, can be used to improve the estimate in (3.2) using $G = \eta_{\mathrm{r}} D$.

The performance of an arbitrary antenna can be compared with the upper bounds in §§3 and 4 using either the MoM or the finite difference time domain method (FDTD). For such a comparison, it is beneficial to determine the integrated extinction and compare the result using (2.3) rather than (3.4) and (4.5). The reason for this is that the full absorption and scattering properties are contained within (2.3) in contrast to (3.4) and (4.5). In fact, (2.3) is the fundamental physical relation and should be the starting point of most analyses.

In addition to the broadband absorption efficiency $\bar{\eta}$, several implications of the present theory remain to be investigated. Future work includes the effect of non-simple connected geometries (array antennas) and its relation to capacitive coupling and additional analysis of classical antennas. From a wireless

communication point of view, it is also interesting to investigate the connection between the present theory and the concept of correlation and capacity in MIMO communication systems. Some of the problems mentioned here will be addressed in forthcoming papers.

The financial support by the Swedish Research Council and the SSF Center for High Speed Wireless Communication are gratefully acknowledged. The authors are also grateful for fruitful discussions with Anders Karlsson and Anders Derneryd at Department of Electrical and Information Technology, Lund University, Sweden.

Appendix A. Details on the derivation of (2.3)

Consider a plane-wave excitation $\boldsymbol{E}_{\mathrm{i}}(\mathrm{c}_0 t - \hat{\boldsymbol{k}}\cdot\boldsymbol{x})$ incident in the $\hat{\boldsymbol{k}}$-direction (figure 1). In the far-field region, the scattered electric field $\boldsymbol{E}_{\mathrm{s}}$, at time t and position $\boldsymbol{x}$, is described by the far-field amplitude $\boldsymbol{F}$ as

$$\boldsymbol{E}_{\mathrm{s}}(t,\boldsymbol{x}) = \frac{\boldsymbol{F}(\mathrm{c}_0 t - x, \hat{\boldsymbol{x}})}{x} + \mathcal{O}(x^{-2}) \quad \text{as} \quad x \to \infty, \tag{A 1}$$

where c_0 denotes the speed of light in a vacuum and $\hat{\boldsymbol{x}} = \boldsymbol{x}/x$ with $x = |\boldsymbol{x}|$. The far-field amplitude $\boldsymbol{F}$ in the forward direction $\hat{\boldsymbol{k}}$ is assumed to be causal and related to the incident field $\boldsymbol{E}_{\mathrm{i}}$ via the linear and time-translational invariant convolution

$$\boldsymbol{F}(\tau,\hat{\boldsymbol{k}}) = \int_{-\infty}^{\tau} \mathbf{S}_{\mathrm{t}}(\tau-\tau',\hat{\boldsymbol{k}},\hat{\boldsymbol{k}})\cdot\boldsymbol{E}_{\mathrm{i}}(\tau')\mathrm{d}\tau'.$$

Here, $\tau = \mathrm{c}_0 t - x$ and $\mathbf{S}_{\mathrm{t}}$ is the appropriate dimensionless temporal dyadic.

Introducing the forward scattering dyadic $\mathbf{S}$ as the Fourier transform of $\mathbf{S}_{\mathrm{t}}$ evaluated in the forward direction, i.e.

$$\mathbf{S}(k,\hat{\boldsymbol{k}}) = \int_{0^-}^{\infty} \mathbf{S}_{\mathrm{t}}(\tau,\hat{\boldsymbol{k}},\hat{\boldsymbol{k}})\mathrm{e}^{\mathrm{i}k\tau}\mathrm{d}\tau, \tag{A 2}$$

where k is complex valued and real-valued with $\mathrm{Re}\, k = \omega/\mathrm{c}_0$. Recall that $\mathbf{S}(\mathrm{i}k,\hat{\boldsymbol{k}})$ is real valued for real-valued k and that the crossing symmetry $\mathbf{S}(k,\hat{\boldsymbol{k}}) = \mathbf{S}^*(-k^*,\hat{\boldsymbol{k}})$ holds for complex-valued k. For a large class of temporal dyadics $\mathbf{S}_{\mathrm{t}}$, the elements of $\mathbf{S}$ are holomorphic in the upper half plane $\mathrm{Im}\, k > 0$.

From the analysis above, it follows that the Fourier transform of (A 1) in the forward direction reads

$$\boldsymbol{E}_{\mathrm{s}}(k, x\hat{\boldsymbol{k}}) = \frac{\mathrm{e}^{\mathrm{i}kx}}{x}\mathbf{S}(k,\hat{\boldsymbol{k}})\cdot\boldsymbol{E}_0 + \mathcal{O}(x^{-2}) \quad \text{as} \quad x\to\infty,$$

where $\boldsymbol{E}_0$ is the Fourier amplitude of the incident field. Introduce the extinction volume $\varrho(k) = \hat{\boldsymbol{p}}_{\mathrm{e}}^*\cdot\mathbf{S}(k,\hat{\boldsymbol{k}})\cdot\hat{\boldsymbol{p}}_{\mathrm{e}}/k^2$, where $\hat{\boldsymbol{p}}_{\mathrm{e}} = \boldsymbol{E}_0/|\boldsymbol{E}_0|$ and $\hat{\boldsymbol{p}}_{\mathrm{m}} = \hat{\boldsymbol{k}}\times\hat{\boldsymbol{p}}_{\mathrm{e}}$ denote the electric and magnetic polarizations, respectively. Since the elements of $\mathbf{S}$ are holomorphic in k for $\mathrm{Im}\, k > 0$, it follows that the extinction volume ϱ is also a holomorphic function in the upper half plane. The Cauchy integral theorem with respect to the contour in figure 6 then yields

$$\varrho(\mathrm{i}\varepsilon) = \int_0^{\pi} \frac{\varrho(\mathrm{i}\varepsilon - \varepsilon\mathrm{e}^{\mathrm{i}\phi})}{2\pi}\,\mathrm{d}\phi + \int_0^{\pi} \frac{\varrho(\mathrm{i}\varepsilon + R\mathrm{e}^{\mathrm{i}\phi})}{2\pi}\,\mathrm{d}\phi + \int_{\varepsilon<|k|<R} \frac{\varrho(k+\mathrm{i}\varepsilon)}{2\pi\mathrm{i}k}\,\mathrm{d}k. \tag{A 3}$$

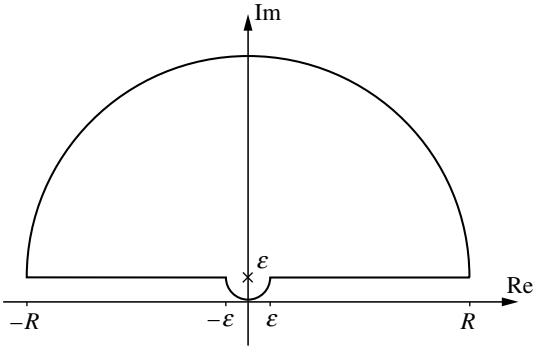

Figure 6. Integration contour in the complex k-plane used in (A 3).

Here, it is assumed that the extinction volume ϱ is sufficiently regular to extend the contour to the real axis in the last integral on the r.h.s. of (A 3). Relation (A 3) is subject to the limits as $\varepsilon \to 0$ and $R \to \infty$.

The l.h.s. of (A 3) and the integrand in the first integral on the r.h.s. are well defined in the limit as $\varepsilon \to 0$. For a sufficiently regular ϱ in the vicinity of the origin, the analysis by Kleinman & Senior (1986) yields

$$\varrho(\mathrm{i}\varepsilon) = \frac{1}{4\pi}(\hat{\boldsymbol{p}}_{\mathrm{e}}^{*} \cdot \boldsymbol{\gamma}_{\mathrm{e}} \cdot \hat{\boldsymbol{p}}_{\mathrm{e}} + \hat{\boldsymbol{p}}_{\mathrm{m}}^{*} \cdot \boldsymbol{\gamma}_{\mathrm{m}} \cdot \hat{\boldsymbol{p}}_{\mathrm{m}}) + \mathcal{O}(\varepsilon) \quad \text{as } \varepsilon \to 0. \tag{A 4}$$

Here, $\boldsymbol{\gamma}_{\mathrm{e}}$ and $\boldsymbol{\gamma}_{\mathrm{m}}$ denote the electric and magnetic polarizability dyadics (see appendix B). Since the short-wavelength response of a material is non-unique from a modelling point of view by Gustafsson (2003), the second term on the r.h.s. of (A 3) is assumed to approach zero in the limit $R \to \infty$. In fact, for a large class of temporal dyadics $\mathbf{S}_{\mathrm{t}}$, the integrand $\varrho(\mathrm{i}\varepsilon + R\mathrm{e}^{\mathrm{i}\phi})/2\pi$ is proportional to the projected area A in the forward direction, namely

$$\varrho(k) = -\frac{A(\hat{\boldsymbol{k}})}{2\pi \mathrm{i} k} + \mathcal{O}(|k|^{-2}) \quad \text{as } |k| \to \infty, \qquad \operatorname{Im} k \geq 0. \tag{A 5}$$

The asymptotic behaviour (A 5) is known as the extinction paradox (see van de Hulst 1957). The constant A is real valued since $\mathbf{S}(\mathrm{i}k, \hat{\boldsymbol{k}})$ is real valued for real-valued k.

In order to proceed, the scattering, absorption and extinction cross-sections are introduced. The scattering cross-section σ_{s} and absorption cross-section σ_{a} are defined as the ratio of the scattered and absorbed power, respectively, to the incident power flow density in the forward direction. The sum of the scattering and absorption cross-sections is the extinction cross-section $\sigma_{\mathrm{ext}} = \sigma_{\mathrm{s}} + \sigma_{\mathrm{a}}$. The three cross-sections σ_{s}, σ_{a} and σ_{ext} are by definition real-valued and non-negative. The principle of energy conservation takes the form as a relation between the extinction volume ϱ and the extinction cross-section. The relation is known as the optical theorem (Newton (1982) and Taylor (1983)),

$$\sigma_{\mathrm{ext}}(k) = 4\pi k \operatorname{Im} \varrho(k), \tag{A 6}$$

where k is real-valued.

In summary, the real part of (A 3) subject to the limits $\varepsilon \to 0$ and $R \to \infty$ yields

$$\varrho(0) = \frac{1}{\pi} \int_{-\infty}^{\infty} \frac{\operatorname{Im} \varrho(k)}{k} \, \mathrm{d}k. \tag{A 7}$$

The optical theorem (A 6) applied to (A 7) then implies

$$\varrho(0) = \frac{1}{4\pi^2} \int_{-\infty}^{\infty} \frac{\sigma_{\mathrm{ext}}(k)}{k^2} \, \mathrm{d}k = \frac{1}{4\pi^3} \int_0^{\infty} \sigma_{\mathrm{ext}}(\lambda) \, \mathrm{d}\lambda, \tag{A 8}$$

where the wavelength $\lambda = 2\pi/k$ has been introduced. Hence, (A 4) inserted into (A 8) yields the integrated extinction

$$\int_0^{\infty} \sigma_{\mathrm{ext}}(\lambda) \, \mathrm{d}\lambda = \pi^2 (\hat{\boldsymbol{p}}_{\mathrm{e}}^* \cdot \boldsymbol{\gamma}_{\mathrm{e}} \cdot \hat{\boldsymbol{p}}_{\mathrm{e}} + \hat{\boldsymbol{p}}_{\mathrm{m}}^* \cdot \boldsymbol{\gamma}_{\mathrm{m}} \cdot \hat{\boldsymbol{p}}_{\mathrm{m}}). \tag{A 9}$$

In fact, the already weak assumptions on the extinction volume ϱ in the analysis above can be relaxed via the introduction of certain classes of distributions (Nussenzveig 1972).

Appendix B. The polarizability dyadics

Let $\boldsymbol{\tau}$ denote a finite material dyadic ($\boldsymbol{\chi}_{\mathrm{e}}$ without a conductivity term or $\boldsymbol{\chi}_{\mathrm{m}}$) with compact support. The entries of the polarizability dyadic $\boldsymbol{\gamma}$ ($\boldsymbol{\gamma}_{\mathrm{e}}$ or $\boldsymbol{\gamma}_{\mathrm{m}}$ depending on whether the problem is electric or magnetic) are defined as the volume integral

$$\hat{\boldsymbol{e}}_i \cdot \boldsymbol{\gamma} \cdot \hat{\boldsymbol{e}}_j = \frac{1}{E_0} \hat{\boldsymbol{e}}_i \cdot \int_{\mathbb{R}^3} \boldsymbol{\tau}(\boldsymbol{x}) \cdot \boldsymbol{E}_j(\boldsymbol{x}) \, \mathrm{d}V_{\boldsymbol{x}}, \quad i, j = 1, 2, 3. \tag{B 1}$$

Here, the total field $\boldsymbol{E}$ has been decomposed as $\boldsymbol{E}_j = E_0 \hat{\boldsymbol{e}}_j + \boldsymbol{E}_{\mathrm{s}j}$ with respect to the mutually orthonormal vectors $\hat{\boldsymbol{e}}_j$. In the electric and magnetic cases, $\boldsymbol{E}$ represents the electric and magnetic fields, respectively.

In the high-contrast limit, when the entries of $\boldsymbol{\tau}$ simultaneously approach infinity uniformly in $\boldsymbol{x}$, the pertinent definition of the high-contrast polarizability dyadic $\boldsymbol{\gamma}_\infty$ is (Kleinman & Senior 1986),

$$\hat{\boldsymbol{e}}_j \cdot \boldsymbol{\gamma}_\infty \cdot \hat{\boldsymbol{e}}_j = \frac{1}{E_0} \hat{\boldsymbol{e}}_i \cdot \sum_{n=1}^{N} \int_{S_n} \hat{\boldsymbol{\nu}}(\boldsymbol{x}) \Phi_j(\boldsymbol{x}) - \boldsymbol{x} \hat{\boldsymbol{\nu}}(\boldsymbol{x}) \cdot \nabla \Phi_j(\boldsymbol{x}) \, \mathrm{d}S_{\boldsymbol{x}}. \tag{B 2}$$

The surface integral representation (B 2) holds for N disjunct bounding surfaces S_n with outward-directed unit normal vectors $\hat{\boldsymbol{\nu}}$. The potential $\Psi_j(\boldsymbol{x}) = \Phi_j(\boldsymbol{x}) - E_0 x_j$ is for each $n = 1, 2, \ldots, N$, the solution to the boundary value problem

$$\begin{cases} \nabla^2 \Psi_j(\boldsymbol{x}) = 0, \quad \boldsymbol{x} \text{ outside } S_n \\ \int_{S_n} \hat{\boldsymbol{\nu}}(\boldsymbol{x}) \cdot \nabla \Psi_j(\boldsymbol{x})|_+ \, \mathrm{d}S_{\boldsymbol{x}} = 0 \\ \Psi_j(\boldsymbol{x}) \to -E_0 x_j + \mathcal{O}(|\boldsymbol{x}|^{-2}) \quad \text{as } |\boldsymbol{x}| \to \infty. \end{cases}$$

The presence of a finite or infinite conductivity term in $\boldsymbol{\chi}_{\mathrm{e}}$ is discussed by Kleinman & Senior (1986). The conclusion is that the electric polarizability dyadic $\boldsymbol{\gamma}_{\mathrm{e}}$ should be replaced by $\boldsymbol{\gamma}_\infty$ independently of the real part of $\boldsymbol{\chi}_{\mathrm{e}}$ when a conductivity

term is present. This may at first seem contradictory, since there is no continuity in the limit as the conductivity vanishes.

In the work by Sohl *et al.* (in press), the polarizability dyadic $\boldsymbol{\gamma}$ is proved to be symmetric provided $\boldsymbol{\tau}$ is symmetric at all points $\boldsymbol{x}$. The dyadic $\boldsymbol{\gamma}$ is real-valued and hence diagonalizable with real-valued eigenvalues. The corresponding set of orthogonal eigenvectors is the principal axes of the obstacle under consideration. The principal axes are particularly easy to determine for obstacles with continuous or discrete symmetries, e.g. the ellipsoids and the Platonic solids by Gustafsson *et al.* (2007).

An important property of $\boldsymbol{\gamma}$ which is proved by Sohl *et al.* (in press) is that it is proportional to the volume of the support of $\boldsymbol{\tau}$. This is a direct consequence of the absence of any length scales in the long-wavelength limit.

Appendix C. The depolarizing factors

For the ellipsoids of revolution, i.e. the prolate and oblate spheroids, closed-form expressions of (6.2) exist in terms of the semi-axis ratio $\xi \in [0,1]$. The result for the prolate spheroid is ($a_2 = a_3$)

$$\begin{cases} L_1(\xi) = \dfrac{\xi^2}{2(1-\xi^2)^{3/2}} \left(\ln \dfrac{1+\sqrt{1-\xi^2}}{1-\sqrt{1-\xi^2}} - 2\sqrt{1-\xi^2} \right) \\ L_2(\xi) = L_3(\xi) = \dfrac{1}{4(1-\xi^2)^{3/2}} \left(2\sqrt{1-\xi^2} - \xi^2 \ln \dfrac{1+\sqrt{1-\xi^2}}{1-\sqrt{1-\xi^2}} \right) \end{cases}, \tag{C 1}$$

while for the oblate spheroid ($a_1 = a_2$)

$$\begin{cases} L_1(\xi) = L_2(\xi) = \dfrac{\xi^2}{2(1-\xi^2)} \left(-1 + \dfrac{\arcsin\sqrt{1-\xi^2}}{\xi\sqrt{1-\xi^2}} \right) \\ L_3(\xi) = \dfrac{1}{1-\xi^2} \left(1 - \dfrac{\xi \arcsin\sqrt{1-\xi^2}}{\sqrt{1-\xi^2}} \right) \end{cases}. \tag{C 2}$$

The depolarizing factors (C 1) and (C 2) are depicted in figure 7. Note that (C 1) and (C 2) differ in indices from the depolarizing factors by Sohl *et al.* (in press) due to the order relation $L_1 \leq L_2 \leq L_3$ assumed in §6 of this paper.

Introduce the eigenvalues $\gamma_j(\xi) = V(\xi)/L_j(\xi)$ of the high-contrast polarizability dyadic. In terms of the radius a of the smallest circumscribing sphere, the spheroidal volume $V(\xi)$ is given by $\xi^2 4\pi a^3/3$ and $\xi 4\pi a^3/3$ for the prolate and oblate spheroids, respectively. For the analysis in §6, the limit of $\gamma_j(\xi)$ as $\xi \to 0$ is particularly interesting, corresponding to the circular needle for the prolate spheroid and the circular disc for the oblate spheroid. The result for the circular

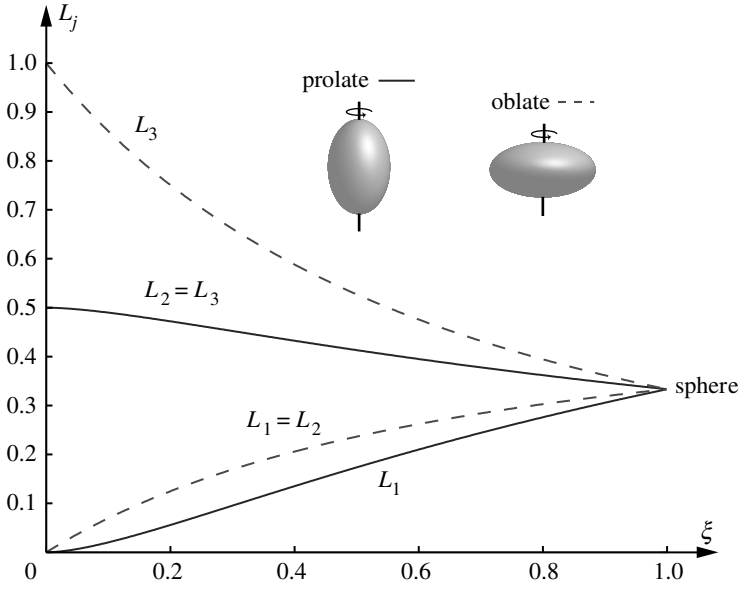

Figure 7. The depolarizing factors for the prolate and oblate spheroids as function of the semi-axis ratio ξ. Note the degeneracy for the sphere.

needle reads

$$\begin{cases} \gamma_1(\xi) = \dfrac{4\pi a^3}{3}\dfrac{1}{\ln 2/\xi - 1} + \mathcal{O}(\xi^2) \\ \gamma_2(\xi) = \gamma_3(\xi) = \mathcal{O}(\xi^2) \end{cases} \quad \text{as } \xi \to 0, \tag{C 3}$$

while for the circular disc

$$\begin{cases} \gamma_1(\xi) = \gamma_2(\xi) = \dfrac{16a^3}{3} + \mathcal{O}(\xi) \\ \gamma_3(\xi) = \mathcal{O}(\xi) \end{cases} \quad \text{as } \xi \to 0. \tag{C 4}$$

Closed-form expressions of (6.2) can also be evaluated for the elliptic needle and disc in terms of the complete elliptic integrals of the first and second kind (see Sohl *et al.* (in press)).

References

Andersen, J. B. & Frandsen, A. 2005 Absorption efficiency of receiving antennas. *IEEE Trans. Antennas Propag.* **53**, 2843–2849. (doi:10.1109/TAP.2005.854532)

Chu, L. J. 1948 Physical limitations of omni-directional antennas. *Appl. Phys.* **19**, 1163–1175. (doi:10.1063/1.1715038)

Elliott, R. S. 2003 *Antenna theory and design*. New York, NY: IEEE Press. Revised edition.

Fano, R. M. 1950 Theoretical limitations on the broadband matching of arbitrary impedances. *J. Franklin Inst.* **249**, 57–83 see also 139–154. (doi:10.1016/0016-0032(50)90006-8)

Gustafsson, M. 2003 On the non-uniqueness of the electromagnetic instantaneous response. *J. Phys. A Math. Gen.* **36**, 1743–1758. (doi:10.1088/0305-4470/36/6/317)

Gustafsson, M. & Nordebo, S. 2006 Bandwidth, *Q*-factor, and resonance models of antennas. *Prog. Electromagn. Res.* **62**, 1–20. (doi:10.2528/PIER06033003)

Gustafsson, M., Sohl, C. & Kristensson, G. 2007 Physical limitations on antennas of arbitrary shape. Technical report LUTEDX/(TEAT-7153)/1-37/(2007), Department of Electrical and Information Technology, Lund University, P.O. Box 118, S-221 00 Lund, Sweden. See http://www.eit.lth.se.

Hansen, R. C. 2006 *Electrically small, superdirective, and superconductive antennas*. New Jersey, NJ: Wiley.

IEEE 1993 IEEE standard definitions of terms for antennas. IEEE Std 145-1993. ISBN 1-55937-31-2.

Kleinman, R. E., Senior, T. B. A., 1986 Rayleigh scattering. In *Low and high frequency asymptotics*, vol. 2 (eds V. V. Varadan V. K. Varadan), ch.1, pp. 1–70. Amsterdam, The Netherlands: Elsevier Science.

Newton, R. G. 1982 *Scattering theory of waves and particles*. New York, NY: Springer.

Nussenzveig, H. M. 1972 *Causality and dispersion relations*. London, UK: Academic Press.

Silver, S. 1949 Microwave antenna theory and design. Radiation laboratory series, vol. 12. New York, NY: McGraw-Hill.

Sohl, C., Gustafsson, M. & Kristensson, G. In press. Physical limitations on broadband scattering by heterogeneous obstacles. *J. Phys. A: Math. Theor.*

Sohl, C., Gustafsson, M. & Kristensson, G. 2007 Physical limitations on metamaterials: restrictions on scattering and absorption over a frequency interval. Technical report LUTEDX/(TEAT-7154)/1-15/(2007), Department of Electrical and Information Technology, Lund University, P.O. Box 118, S-221 00 Lund, Sweden. See http://www.eit.lth.se.

Taylor, J. R. 1983 *Scattering theory: the quantum theory of nonrelativistic collisions*. Malabar, FL: Robert E. Krieger Publishing Company.

van de Hulst, H. 1957 *Light scattering by small particles*. New York, NY: Wiley.

Wheeler, H. A. 1947 Fundamental limitations of small antennas. *Proc. IRE* **35**, 1479–1484. (doi:10.1109/JRPROC.1947.226199)

Yaghjian, A. D. & Best, S. R. 2005 Impedance, bandwidth, and *Q* of antennas. *IEEE Trans. Antennas Propag.* **53**, 1298–1324. (doi:10.1109/TAP.2005.844443)